Electronic Supplementary Material: Polymer Chain with Dipolar Active Forces in Connection to Spatial Organization of Chromatin

Subhasish Chaki,[1, 2, *] Ligesh Theeyancheri,[2, †] and Rajarshi Chakrabarti[2, ‡]
[1] *Department of Materials Science and Engineering,*
University of Illinois, Urbana, Illinois - 61801, USA
[2] *Department of Chemistry, Indian Institute of Technology Bombay, Mumbai, Maharashtra - 400076, India*

I. MEAN SQUARE DISPLACEMENT OF THE CENTER OF MASS

The most straightforward tool for understanding the properties of motion from the trajectories is the mean square displacement (MSD). The time-averaged MSD of the center of mass (COM) is defined as $\overline{\Delta r_c^2(\tau)} = \frac{1}{T-\tau}\int_0^{T-\tau}\left[\vec{r}_c(t_0+\tau)-\vec{r}_c(t_0)\right]^2 dt_0$ from the time series of the position of the COM $\vec{r}_c(t)$ where T is the total run time and τ is the lag time. The time-and-ensemble-averaged MSD of the COM is obtained as: $\left\langle \overline{\Delta r_c^2(\tau)} \right\rangle = \frac{1}{N'}\sum_{i=1}^{N'}\overline{\Delta r_c^2(\tau)}$ where N' is the number of independent trajectories. The MSD $\left(\left\langle \overline{\Delta r_c^2(\tau)} \right\rangle\right)$ of the center of mass (COM) diffuses freely at all times in the presence or absence of extensile and contractile activity (Fig. S1). In addition, all the active and passive $\left\langle \overline{\Delta r_c^2(\tau)} \right\rangle$ are merging with each other (Fig. S1). However, in the long time limit, the dynamics of the center of mass of the polymer chain will be obstructed by the spherical confinement (Fig. S2).

II. DISTRIBUTION FUNCTIONS OF THE RADIUS OF GYRATION

To further quantify the effects of the contractile and extensile active forces on the loci mobilities, we analyze the probability distribution, $(P(R_g))$ of the radius of gyration R_g of the chain where $R_g = \sqrt{\frac{1}{\mathrm{N}}\sum_{i=1}^{N}\left(r_i - r_{\mathrm{c}}\right)^2}$. For smaller DPC and DPE activities, $P(R_g)$s are Gaussian and appear to be qualitatively similar to $P(R_g)$ of passive system. But, $P(R_g)$s for high DPE and DPC forces show well-separated peaks (Fig. S4). For large DPC force, $P(R_g)$ is Gaussian and sharply peaked at lower values of R_g. The broader distribution of $P(R_g)$ with peak at higher value of R_g deviates from the Gaussian for large DPE force which accounts for the enhancement of stretching of the polymer chain. For the high DPC force, the deviation of the peak value of $P(R_g)$ from the passive case is small as compared to the deviation for the DPE force. This small deviation for the DPC force is most probably due to the self-avoidance of the beads. To test the effect of self-avoidance as an energetic barrier, we compute the potential energy and the mean square fluctuation of the velocity (v), $\langle v^2 \rangle$ per particle of the polymer chain at each instant of time in the steady state. The velocity of a monomer over the integration time step δt is defined as $v = \frac{\vec{r}_n(t+\delta t)-\vec{r}_n(t)}{\delta t}$. It is a quantity that can be measured experimentally by tracking the position of a chromosomal locus as a function of time [1] and has been extensively used to determine the nature of the stochastic process underlying the observed motion [2, 3]. PE per particle increases more for the DPC forces than for the DPE forces (Fig. S3A) as the effect of self-avoidance translates to an increasing potential energy barrier for the DPC forces. On the other hand, $\langle v^2 \rangle$ per particle increases more for the DPE forces than for the contractile forces (Fig. S3B) as the DPE forces show larger displacements than the DPC forces.

III. NUMBER FLUCTUATIONS

To gain a deeper understanding of the underlying complex movement of the monomers, we investigate the number fluctuations. To compute the number fluctuations, we randomly select a number of small spherical probes of radius 4σ at different locations within the system. We then construct a histogram over different spherical probes and independent trajectories from which probabilities $(P(N))$ are computed. In equilibrium, the statistics of fluctuations in N inside a small spherical probe volume follows Gaussian distribution. For small values of DPE and DPC forces, we find that the the probability distributions $P(N)$ are indeed Gaussian (Fig. S5). For large DPC force, $P(N)$ also exhibits the Gaussian distribution. For large DPC force, the peak of $P(N)$ shifts towards a higher value of N and the width of $P(N)$ becomes narrower than the passive one (Fig. S5). Hence, large DPC force generates high density regions, leading to decrease in mobility. On contrary, for large DPE force, $P(N)$ decays exponentially with N, indicating that DPE forces promote larger displacements of the system than the passive one.

---

[*] subhasischaki@gmail.com
[†] ligeshbhaskar@gmail.com
[‡] rajarshi@chem.iitb.ac.in

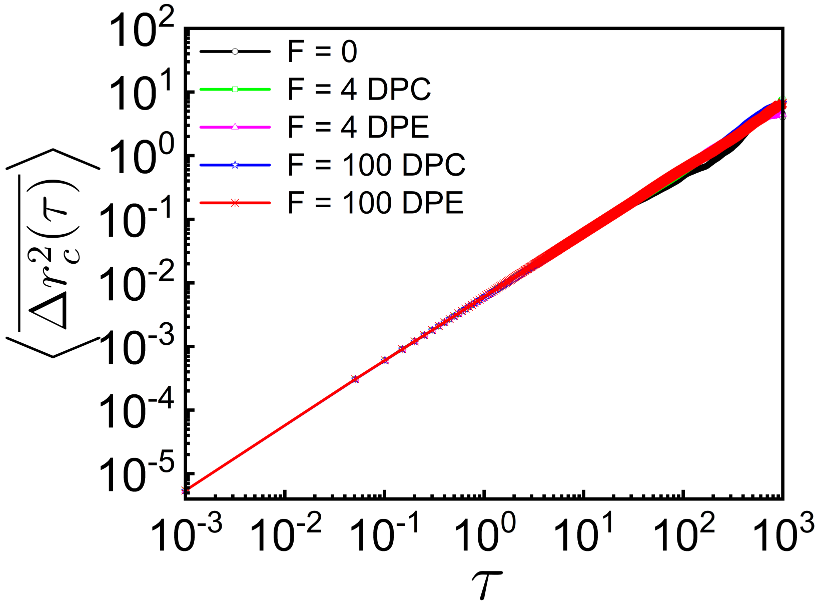

FIG. S1. Log-Log plot of MSDs $\left(\left\langle \overline{\Delta r_c^2(\tau)} \right\rangle\right)$ as a function of lag time τ at different DPE and DPC active forces for the COM of polymer chain.

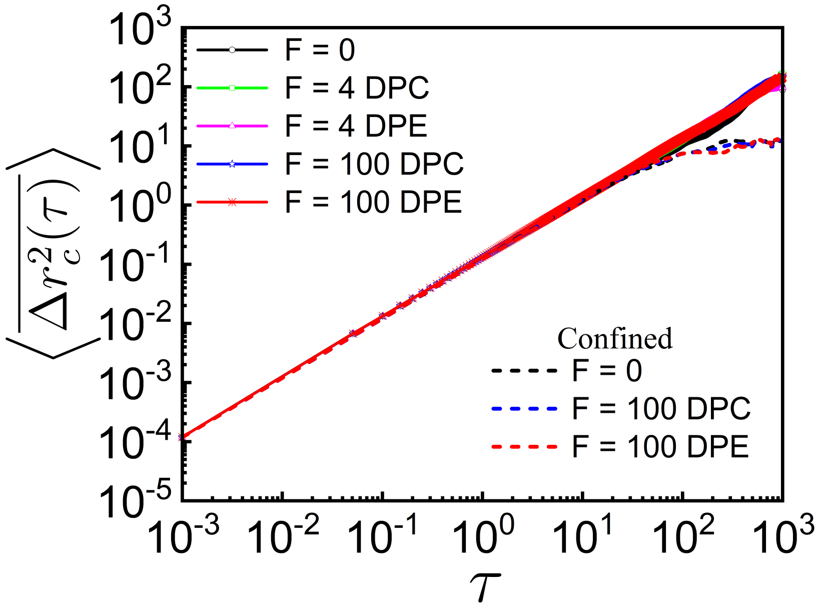

FIG. S2. Log-Log plot of MSDs $\left(\left\langle \overline{\Delta r_c^2(\tau)} \right\rangle\right)$ as a function of lag time τ at different DPE and DPC active forces for the COM of polymer chain under spherical confinement.

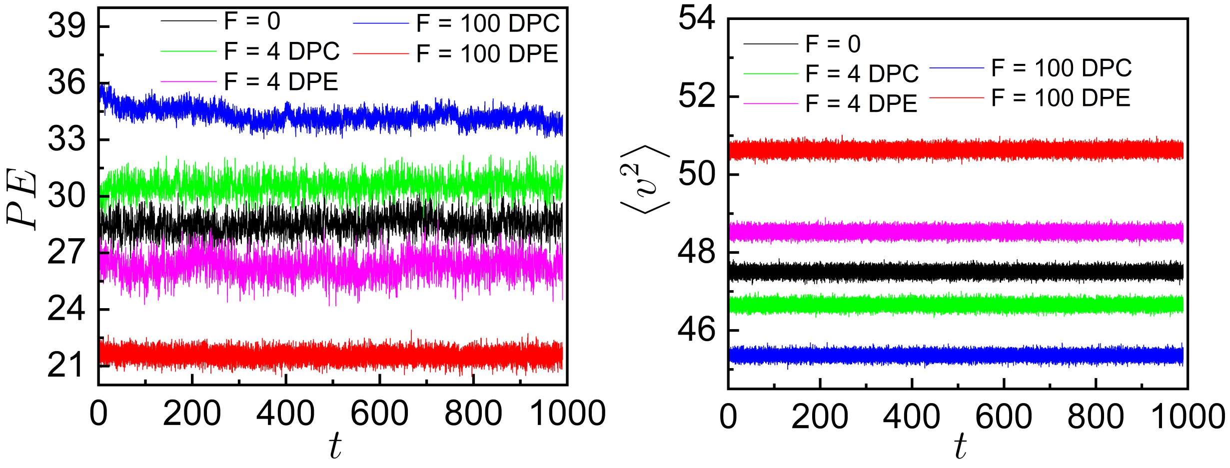

(A)

(B)

FIG. S3. Steady state PE per particle (A) and $\langle v^2 \rangle$ per particle (B) as a function of time t at different DPE and DPC active forces for polymer chain.

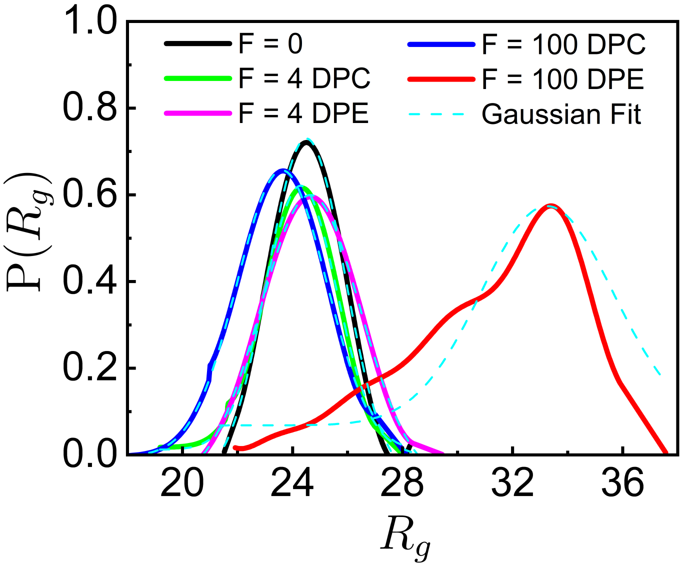

FIG. S4. The probability distribution function ($P(R_g)$) of the radius of gyration (R_g) in the presence of at different DPE and DPC active forces.

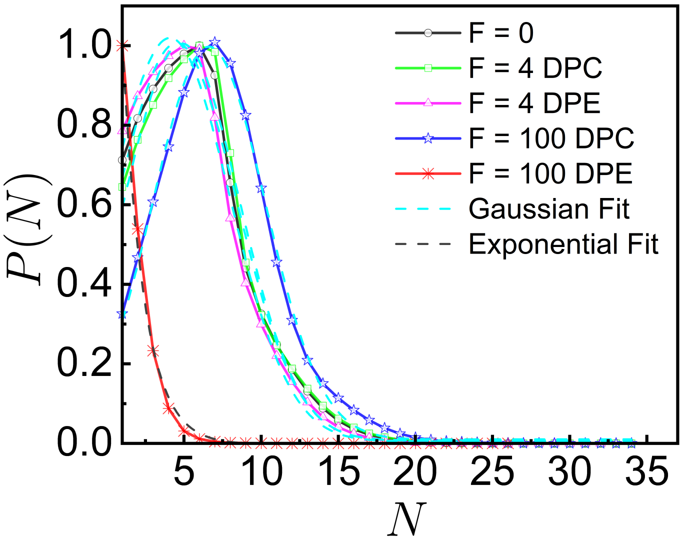

FIG. S5. Number density fluctuations ($P(N)$) at different DPE and DPC activities..

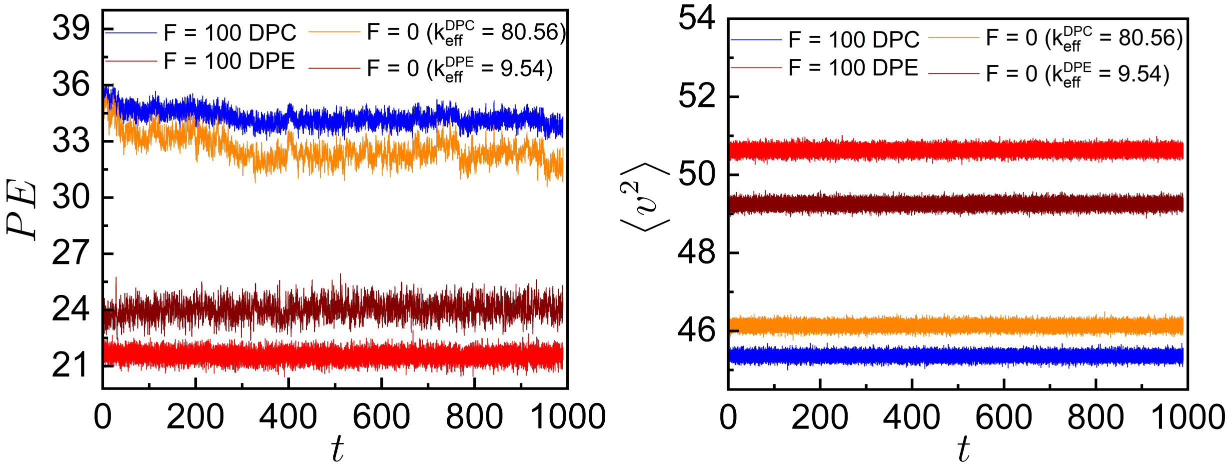

(A) (B)

FIG. S6. Steady state PE per particle (A) and $\langle v^2 \rangle$ per particle (B) as a function of time t for the thermal chain with effective spring constants $k_{\text{eff}}^{\text{DPE}}$ and $k_{\text{eff}}^{\text{DPC}}$ and large DPE and DPC dipolar active forces.

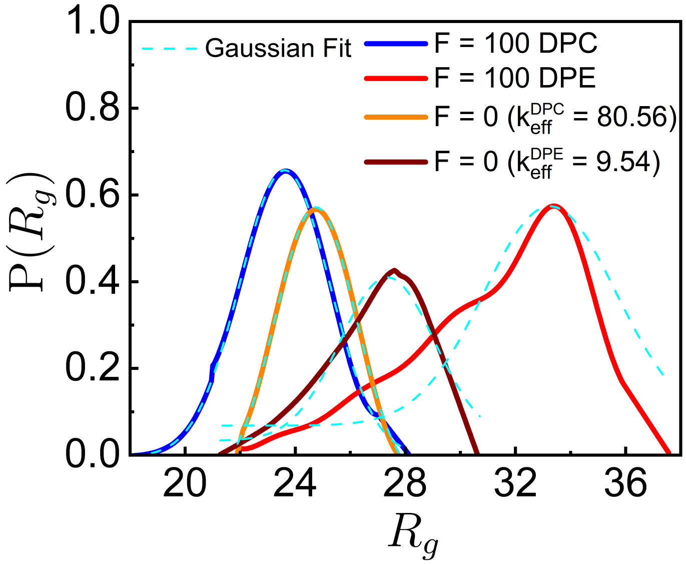

FIG. S7. The probability distribution function ($P(R_g)$) of the radius of gyration (R_g) for the thermal chain with effective spring constants $k_{\rm eff}^{\rm DPE}$ and $k_{\rm eff}^{\rm DPC}$ and large DPE and DPC dipolar active forces.

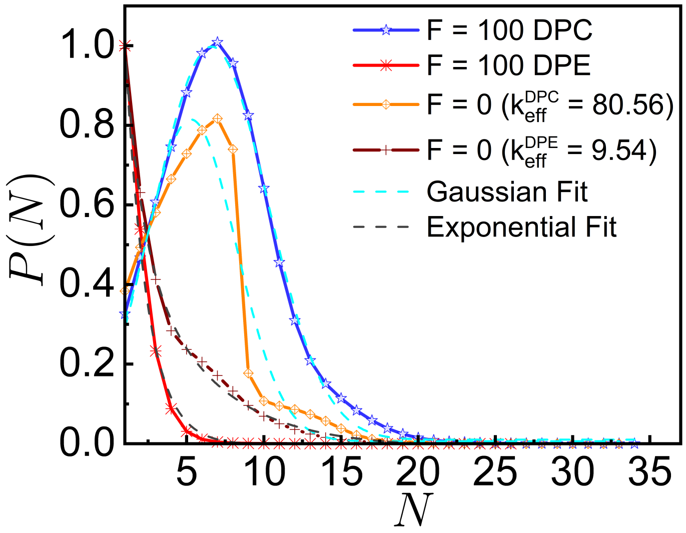

FIG. S8. Number density fluctuations ($P(N)$) for the thermal chain with effective spring constants $k_{\rm eff}^{\rm DPE}$ and $k_{\rm eff}^{\rm DPC}$ and large DPE and DPC dipolar active forces.

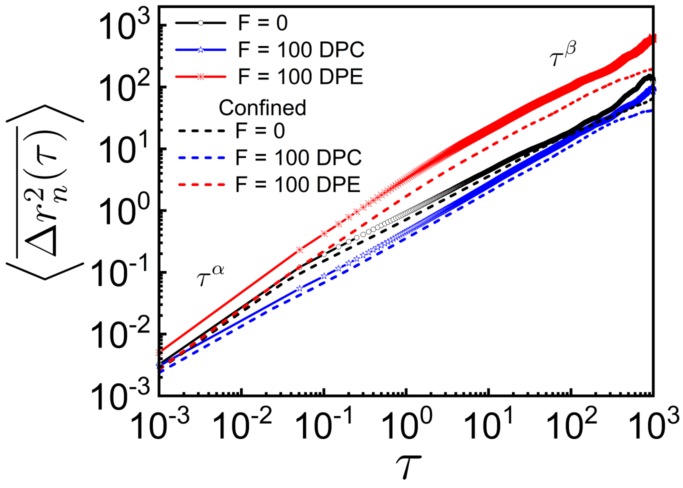

FIG. S9. Log-Log plot of tagged monomer MSDs $\left(\left\langle\overline{\Delta r_n^2(\tau)}\right\rangle\right)$ as a function of lag time τ for the passive, DPE and DPC activities with (dotted lines) and without (solid lines) spherical confinement.

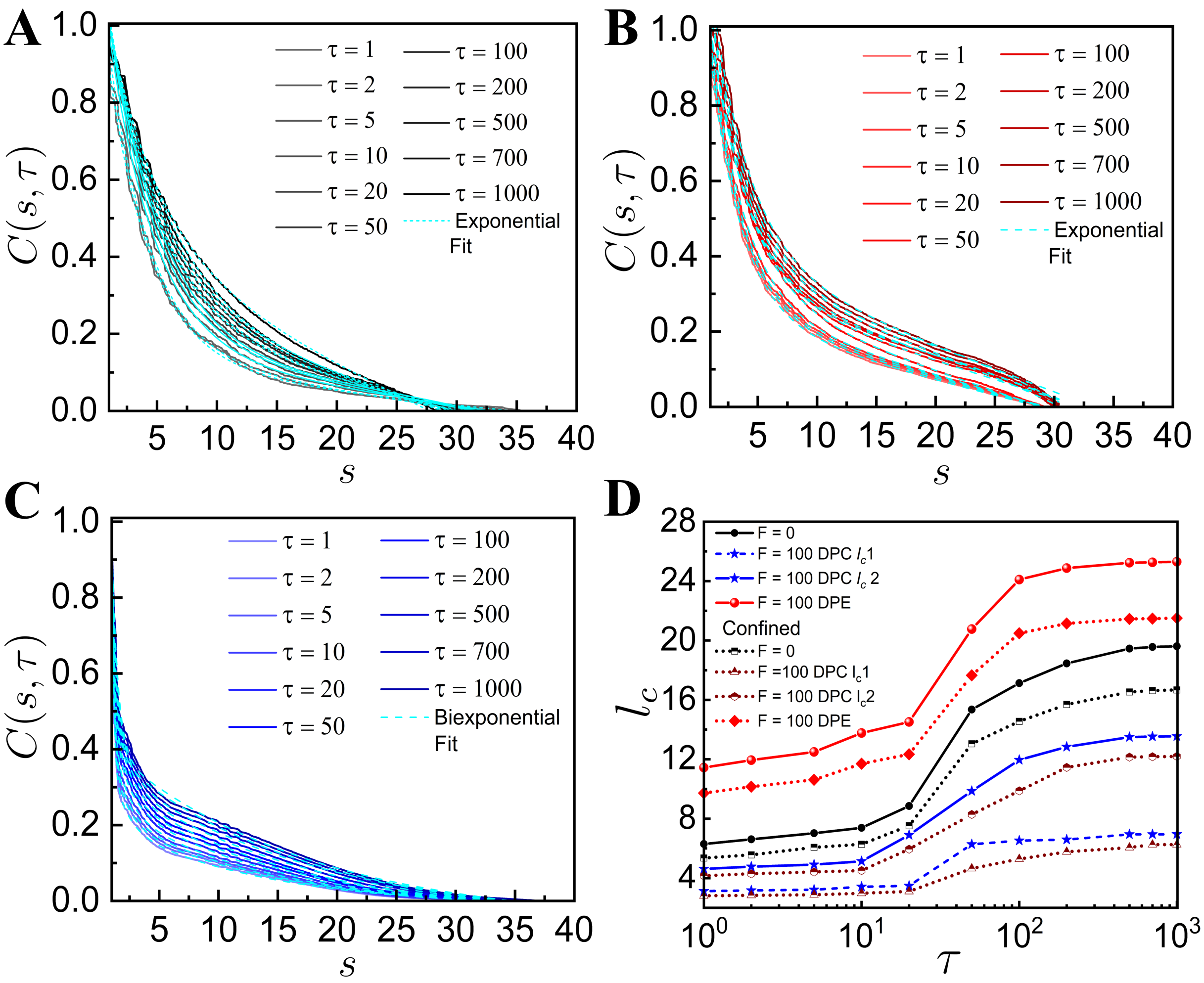

FIG. S10. Spatial correlation functions $C(s,\tau)$ for the passive (A), DPE and DPC cases for F = 100 (B and C) respectively at different time lags, τ under sperical confinement. (D) Correlation lengths (l_c) as a function of τ for the passive, DPE and DPC activities with (dotted lines) and without (solid lines) spherical confinement.

F	α	β
0	0.88	0.77
4 (DPE)	0.88	0.65
4 (DPC)	0.89	0.63
100 (DPE)	0.93	0.68
100 (DPC)	0.74	0.67

TABLE S1. The exponents, α and β of $\left\langle\overline{\Delta r_n^2(\tau)}\right\rangle$ at short and long times for the passive and different dipolar activities.

[1] T. J. Lampo, A. S. Kennard, and A. J. Spakowitz, Physical modeling of dynamic coupling between chromosomal loci, Biophys. J. **110**, 338 (2016).

[2] S. Put, T. Sakaue, and C. Vanderzande, Active dynamics and spatially coherent motion in chromosomes subject to enzymatic force dipoles, Phys. Rev. E **99**, 032421 (2019).

[3] M. Di Pierro, D. A. Potoyan, P. G. Wolynes, and J. N. Onuchic, Anomalous diffusion, spatial coherence, and viscoelasticity from the energy landscape of human chromosomes, Proc. Nat. Acad. Sci. USA **115**, 7753 (2018).